doi:10.3772/j.issn.1006-6748.2024.03.004

Trajectory compensation for multi-robot coordinated lifting system considering elastic catenary of the rope①

ZHAO Xiangtang (赵祥堂), ZHAO Zhigang②, SU Cheng, MENG Jiadong, WANG Baoxi
(School of Mechanical Engineering, Lanzhou Jiaotong University, Lanzhou 730070, P. R. China)

Abstract

The multi-robot coordinated lifting system is an unconstrained system with a rigid and flexible coupling. The deformation of the flexible rope causes errors in the movement trajectory of the lifting system. Based on the kinematic and dynamic analysis of the lifting system, the elastic catenary model considering the elasticity and mass of the flexible rope is established, and the effect of the deformation of the flexible rope on the position and posture of the suspended object is analyzed. According to the deformation of flexible rope, a real-time trajectory compensation method is proposed based on the compensation principle of position and posture. Under the lifting task of the low-speed movement, this is compared with that of the system which neglects the deformation of the flexible rope. The trajectoy of the lifting system considering the deformation of flexible rope. The results show that the mass and elasticity of the flexible rope can not be neglected. Meanwhile, the proposed trajectory compensation method can improve the movement accuracy of the lifting system, which verifies the effectiveness of this compensation method. The research results provide the basis for trajectory planning and coordinated control of the lifting system.

Key words: multi-robot lifting system, deformation of flexible rope, elastic catenary model, compensation principle of position and posture, trajectory compensation

0 Introduction

Compared with traditional rigid parallel robots, rope-driven parallel robots have the advantages of simple structure, large workspace, high payload and small movement inertia, so the rope-driven parallel robots have a wide range of application fields and important research value[1]. The multi-robot coordinated lifting system is a special kind of rope-driven parallel robot that can significantly reduce the weight and inertia of the system by using ropes to drive the suspended object. At present, the rope is simplified into an ideal rod unit in the rope-driven parallel robots, but the rope has obvious droop under the influence of its weight, and the shape of the rope is approximately catenary rather than straight. In addition, the rope is elastic and will stretch under tension, directly ignoring the mass and elasticity of the rope will make the error of the model too large, so that the movement accuracy of the end-effector can not meet the requirements[2-3]. Therefore, it is necessary to consider the mass and elasticity of the rope and establish a dynamic model that satisfies the accuracy requirements.

Existing studies have simplified the dynamic model of the rope-driven parallel robot to the end-effector model for analysis, but only a few studies have considered the elasticity and mass of the rope. Sui et al.[4] simplified the rope into a spring and established a dynamic model of a rope-driven robotic arm. Huang et al.[5] regarded the rope as a point of elastic massless series connection and established the rope model of the space robot. Bedoustani et al.[6] considered the elasticity of the rope and established a dynamic model of the rope-driven parallel manipulator. The aforementioned studies analyzed the movement characteristics of the rope-driven parallel robots but neglected the influence of the rope mass on the movement trajectory. Zhao et al.[7] established the catenary model of the rope considering the mass of the rope, and solved the deformation of the rope by an iterative method. Then, the parabolic model[8] of the rope was established. Yan and Shang[9] used the

① Supported by the National Natural Science Foundation of China (No. 51965032), the Natural Science Foundation of Gansu Province of China (No. 22JR5RA319), the Science and Technology Foundation of Gansu Province of China (No. 21YF5WA060) and the Excellent Doctoral Student Foundation of Gansu Province of China (No. 23JRRA842).

② To whom correspondence should be addressed. E-mail: zhaozhg@mail.lzjtu.cn.

Received on Aug. 14, 2023

catenary model of the rope to analyze the mechanical characteristics of a rope-driven parallel robot, and verified the correctness of the dynamic model through simulation. Based on analyzing the force of the rope, the above studies only give parabolic or catenary models of the rope, and do not deeply study the influence of the catenary model of the rope on the end-effector.

Since the rope can not accurately control the position and posture of the suspended object like a rigid body, the elastic catenary model of the rope needs to be established to dynamically compensate for the deformation of the rope during the lifting, so that the movement of the suspended object tends to the desired movement trajectory. Korayem et al. [10-12] used robust control and sliding mode control to compensate for the deformation of the rope in the rope-driven parallel robot. He et al. [13] used the software compensation method to compensate for the error caused by rope deformation, and the results show that the method can reduce the error of the end-effector. Riehl et al. [14] analyzed the influence of the mass and elasticity of the rope on the end position, and carried out the error compensation in the joint space. The aforementioned studies have improved the tracking performance of rope-driven parallel robots by compensating for the error due to the deformation of the rope. However, error compensation has mainly been studied for single robots and mostly for rigid-body robots.

For the multi-robot coordinated lifting system, the span of the rope is large, the weight of the suspended object is heavy, and it may break suddenly during the lifting, which is potentially dangerous. To improve the movement accuracy of the multi-robot coordinated lifting system, rope deformation caused by the mass and elasticity of the rope should be considered, and the trajectory compensation method should be used to compensate for the trajectory of the lifting system. Firstly, the kinematic and dynamic models of the multi-robot coordinated lifting system are established. Secondly, the elastic catenary model is developed that takes into account the mass and elasticity of the rope. Then, using the mathematical principle of relative position and posture compensation, the trajectory compensation scheme of the lifting system is designed. Finally, the trajectory of the lifting system considering the mass and elasticity of the rope is calculated through the simulation experiment, and the validity of the compensation method is verified. Compared with previous studies, the contribution of this paper is to establish an elastic catenary model that considers both rope mass and elasticity, which makes the rope model more accurate. The proposed trajectory compensation method will help to improve the movement accuracy of the rope-driven parallel robot, and the research results will be useful for practical applications in lifting system.

1 System configuration

The multi-robot coordinated lifting system consists of multiple lifting robots and the rope-driven parallel lifting system. The spatial configuration of the lifting system designed for heavy object transportation in the industry is shown in Fig. 1. The lifting robot consists of a fixed base and a 3-degree of freedom (DOF) joint manipulator, where link 1 can be rotated around the z axis, and links 2 and 3 can be rotated up and down around their joints. The suspended object is connected to the end of the robot by ropes and is suspended under the three robots. The spatial relative positions of the three robots can be designed in real-time according to different application conditions.

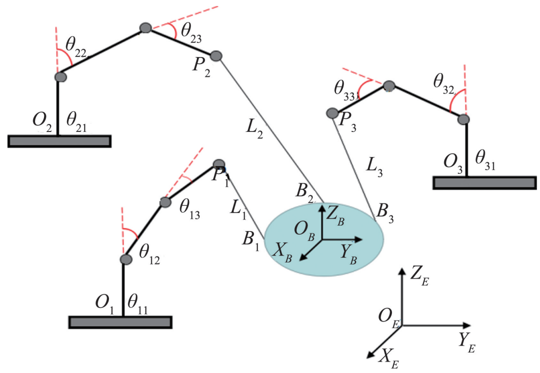

Fig. 1 Spatial configuration of the lifting system

According to the spatial structure of the lifting system, the following coordinate systems are established. The inertial coordinate system O_E is established at a point on the horizontal plane, the coordinate system O_i is established at the bottom of the robot, and the coordinate system O_B is established at the center of the suspended object. The rod length of the robot is a_{i1}, a_{i2}, a_{i3}, the joint angle is $\theta_{i1}, \theta_{i2}, \theta_{i3}$, the position of the connection point between the end of the robot and the rope is $\boldsymbol{P}_i$, the position of the connection point between the rope and the suspended object is $\boldsymbol{B}_i$, the position vector of the rope is $\boldsymbol{L}_i$, the position and posture of the suspended object are $(x, y, z, \alpha, \beta, \gamma)$. Since the whole system is composed of three lifting robots, so $i = 1, 2, 3$.

Due to the complex structure of the actual lifting system, to ensure the stability of the multi-robot coordinated lifting system, the following assumptions are made in the analysis without affecting the analysis results.

(1) The robots are evenly distributed, the ends of the robots do not overlap, and the ropes do not intertwine with each other.

(2) The tension of the rope must be between the minimum preload force and the maximum allowable force to avoid the virtual pull and fracture of the rope.

(3) The structural stiffness of the robot is strong enough, without considering the elastic vibration and deformation after the end of the robot is stressed.

2 Kinematic analysis

When analyzing the forward kinematics of the lifting system, the kinematics of the robot are analyzed first, and then the relationship between the end of the robot and the suspended object is established by taking the end position of the robot and the length of the rope as the intermediate variables. When analyzing the inverse kinematics, the movement state of the suspended object is known, and the inverse kinematics of the suspended object and the end of the robot are first analyzed. After the end position of the robot is obtained, the inverse kinematics of the robot is solved, and the angle of each joint is obtained.

When the lifting robot is not pulled by the rope, the end position of the robot is solved using the Denavit-Hartenberg (D-H) transformation in the coordinate system O_i as follows.

$$\begin{bmatrix} x_{pi} \\ y_{pi} \\ z_{pi} \end{bmatrix} = \begin{bmatrix} a_{i2}\cos\theta_{i1}\cos\theta_{i2} + a_{i3}\cos\theta_{i1}\cos(\theta_{i2} + \theta_{i3}) \\ a_{i2}\sin\theta_{i1}\cos\theta_{i2} + a_{i3}\sin\theta_{i1}\cos(\theta_{i2} + \theta_{i3}) \\ a_{i1} + a_{i2}\sin\theta_{i2} + a_{i3}\sin(\theta_{i2} + \theta_{i3}) \end{bmatrix} \quad (1)$$

Eq. (1) represents the relationship between the end position of the robot and the joint angle. On the premise of ensuring reversibility, the expected input of the end of the robot can be obtained by Eq. (1).

For the kinematics of the rope-driven parallel lifting system, in the coordinate system O_E, the position of the connection point between the end of the robot and the rope is $\boldsymbol{P}_i(x_{Pi}\, y_{Pi}\, z_{Pi})$, the position of the connection point between the rope and the suspended object is $\boldsymbol{B}_i(x_{Bi}\, y_{Bi}\, z_{Bi})$, and the center position of the suspended object is $\boldsymbol{r} = [x \quad y \quad z]^{\mathrm{T}}$. In the coordinate system O_B, the position of the connecting point between the suspended object and the rope is $\boldsymbol{B}_i'$, then:

$$\boldsymbol{B}_i = \boldsymbol{R}\boldsymbol{B}_i' + \boldsymbol{r} \quad (2)$$

where, $\boldsymbol{R}$ is the transformation matrix of the coordinate system O_B relative to the coordinate system O_E.

The kinematic equation of the rope-driven parallel lifting system is as follows.

$$\boldsymbol{L}_i = \boldsymbol{P}_i - \boldsymbol{B}_i = \boldsymbol{P}_i - \boldsymbol{R}\boldsymbol{B}_i' - \boldsymbol{r} \quad (3)$$

Then, the length of the rope is

$$L_i = \sqrt{(\boldsymbol{P}_i - \boldsymbol{B}_i)^{\mathrm{T}}(\boldsymbol{P}_i - \boldsymbol{B}_i)} \quad (4)$$

Eqs (3) and (4) describe the kinematics of the lifting system under ideal conditions, because the mass and elastic deformation of the rope are neglected in the modeling.

When the suspended object moves according to the desired trajectory, the end of the robot and the length of the rope make corresponding changes, and these changes have a variety of cases, namely, the inverse kinematics of the lifting system has multiple solutions. In the practical applications of the lifting system, the movement range of the end of the robot is limited, and hence the inverse solution of the lifting system is also limited.

3 Dynamic analysis

The balance equation of the suspended object is

$$\boldsymbol{J}^{\mathrm{T}}\boldsymbol{T} = \boldsymbol{F} \quad (5)$$

where, $\boldsymbol{J}^{\mathrm{T}} = [J_1 \quad J_2 \quad J_3]$ is the structural matrix of the lifting system:

$$J_i = \begin{bmatrix} \boldsymbol{e}_i \\ (\boldsymbol{R}\boldsymbol{B}_i') \times \boldsymbol{e}_i \end{bmatrix} (i = 1, 2, 3) \quad (6)$$

where, $\boldsymbol{e}_i = \boldsymbol{L}_i / \| \boldsymbol{L}_i \|$ is the unit length vector of the rope.

In Eq. (5), $\boldsymbol{F}$ is the external force-spinor of the suspended object.

$$\boldsymbol{F} = \left[\left(M\frac{\mathrm{d}v}{\mathrm{d}t} \right)^{\mathrm{T}}, \left([D_x, D_y, D_z]\frac{\mathrm{d}\omega}{\mathrm{d}t} \right)^{\mathrm{T}} \right]^{\mathrm{T}} \quad (7)$$

where, M is the mass of the suspended object; D_x, D_y, D_z are the moment of inertia of the suspended object; v and $\boldsymbol{\omega}$ are the linear velocity and angular velocity of the suspended object, respectively.

In Eq. (5), $\boldsymbol{T} = [T_1 \quad T_2 \quad T_3]^{\mathrm{T}}$ and $\boldsymbol{T}_{\min} \leqslant \boldsymbol{T}_i \leqslant \boldsymbol{T}_{\max}$, $\boldsymbol{T}_{\min}$ and $\boldsymbol{T}_{\max}$ are the minimum preload force and maximum allowable tension of the rope, respectively.

To make the inverse solution of the lifting system available, the kinematics and dynamics of the lifting system should be solved simultaneously, and the tension of each rope should be guaranteed to be positive. However, the structure matrix of the lifting system is not square, and the rope tension can not be obtained from the null space matrix $\boldsymbol{N}(\boldsymbol{J}^{\mathrm{T}})$ of the structure matrix. According to the principle of vector closure, the gravity and inertia force of the suspended object are regarded as a virtual rope, and the virtual rope provides tension for the suspended object[15]. Therefore, the tension of the rope needs to be calculated through the generalized inverse of the matrix, then the tension of the rope is

$$\boldsymbol{T} = \boldsymbol{T}_s + \boldsymbol{T}_n = \boldsymbol{J}^+ \boldsymbol{F} + \boldsymbol{\lambda} \cdot \boldsymbol{N}(\boldsymbol{J}^{\mathrm{T}}) \tag{8}$$

where, $\boldsymbol{J}^+ = \boldsymbol{J}^{\mathrm{T}} (\boldsymbol{J} \boldsymbol{J}^{\mathrm{T}})^{-1}$ is the generalized inverse matrix of the structure matrix $\boldsymbol{J}^{\mathrm{T}}$, $\boldsymbol{\lambda}$ is any two-dimensional vector, $\boldsymbol{N}(\boldsymbol{J}^{\mathrm{T}})$ is the null space vector of the structure matrix $\boldsymbol{J}^{\mathrm{T}}$, $\boldsymbol{T}_s$ is the unique special solution of Eq. (5), $\boldsymbol{T}_n$ is the general solution of Eq. (5), which does not work to the system but can change the tension distribution of the rope.

In all the solutions of Eq. (8), the one that satisfies the tension limit of the rope is called the feasible solution. When the feasible solution exists, the solution of the rope tension of the lifting system can be summarized as follows: making the suspended object reach the target position under the premise of ensuring the control accuracy, and seeking a group of optimal tension distribution. The optimization model can be described as

$$\begin{cases} \min \ \| \boldsymbol{T} - \boldsymbol{T}_c \|_2 \\ \text{s.t.} \quad \boldsymbol{J}^{\mathrm{T}} \boldsymbol{T} = \boldsymbol{F} \\ \boldsymbol{T}_{\min} \leqslant \boldsymbol{T}_i \leqslant \boldsymbol{T}_{\max} \end{cases} \tag{9}$$

where, $\boldsymbol{T}_c = (\boldsymbol{T}_{\min} + \boldsymbol{T}_{\max})/2$ is the target value of the rope tension. $\boldsymbol{T}_c$ is in the center of the rope tension limit, $\| \boldsymbol{T} - \boldsymbol{T}_c \|_2$ as the optimization objective function, the optimal solution is far away from the boundary value, and the distribution of the rope tension is more concentrated and uniform, which helps to improve the stability of the lifting system[16]. When the feasible solution does not exist, the convex optimization method is used to solve it, and the initial iteration points are calculated separately for different cases.

4 Trajectory compensation

In an actual multi-robot coordinated lifting system, the rope will deform after being stressed. Although the hoist is equipped with an encoder to control the desired rope length, the real-time rope length and the position of the suspended object can not be obtained, so it is necessary to establish a mathematical model of rope deformation in the lifting system[17]. The effects of the rope mass and elasticity on the lifting system should be taken into account simultaneously. Therefore, the elastic catenary model is used to accurately analyze the deformation of the rope, and the trajectory of the suspended object is compensated in real-time by the compensation method.

4.1 Elastic catenary model of the rope

The use of the catenary equation to describe the shape of the rope can reflect the deformation of the rope under the action of the self-weight, thus ensuring the accuracy of the model. Assuming that the rope is working in the linear elastic range during the whole lifting process, the elastic coefficient of the rope is regarded as a constant[18]. The deformation of the rope in the lifting system is the superposition of catenary deformation and elastic deformation, the shape of the rope is solved as a hyperbolic sine function, regardless of the elasticity of the rope. Then in the case of an elastic rope, the coordinates of any point on the rope can be regarded as the corrections in the case of catenary deformation. This problem is equivalent to establishing the elastic catenary model of the rope.

To carry out force analysis on the rope, the rope coordinate system O_n is established, as shown in Fig. 2, where H is the horizontal component of the rope tension, V is the vertical component of the rope tension, l is the Lagrange coordinate of the rope, s is the arc length coordinate of the rope, L_0 is the original length of the rope, G is the weight of the rope, the weight per unit length of the rope is $\frac{G}{L_0}$, T is the tension of the rope.

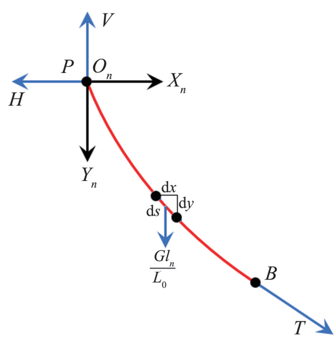

Fig. 2 Flexible rope model

When the lifting task requires the object to move at a low speed, the suspended object is quasi-static, and the rope is subject to its own gravity and external forces T. The rope is divided into n segments, and anyone ds (length is l_n, tension is T_n) of them is taken for analysis. According to the force balance relation, the force balance equation for a segment of a rope micro-element is as follows.

$$\begin{cases} T_n \dfrac{\mathrm{d}x}{\mathrm{d}s} = H \\ T_n \dfrac{\mathrm{d}y}{\mathrm{d}s} = V - \dfrac{Gl_n}{L_0} \end{cases} \tag{10}$$

By the arc length equation in the rectangular coordinate system, the micro-element segment of the rope satisfies the geometric constraints:

$$\left(\frac{\mathrm{d}x}{\mathrm{d}s}\right)^2 + \left(\frac{\mathrm{d}y}{\mathrm{d}s}\right)^2 = 1 \qquad (11)$$

When Eq. (10) is square and then is substituted into Eq. (11), the tension of the rope micro-element segment is

$$T_n = \left[H^2 + \left(V - \frac{Gl_n}{L_0}\right)^2\right]^{\frac{1}{2}} \qquad (12)$$

According to the properties of hyperbolic function and anti-hyperbolic function, the expression[19] of catenary can be solved by using the $T_n = EA_0\left(\frac{\mathrm{d}s}{\mathrm{d}l_n} - 1\right)$ and $\frac{\mathrm{d}x}{\mathrm{d}s} = \frac{\mathrm{d}x}{\mathrm{d}l_n} \cdot \frac{\mathrm{d}l_n}{\mathrm{d}s}$, where E is the elastic modulus of the rope and A_0 is the cross-sectional area.

The elastic deformation Δl_n of the rope is

$$\Delta l_n = \frac{T_n l_n}{EA_0} \qquad (13)$$

When the catenary deformation of the rope is superposed with the elastic deformation, the elastic catenary of the rope is expressed as follows.

$$\begin{cases} x_n = \dfrac{Hl_n}{EA_0} + \dfrac{HL_0}{G}\left[\sinh^{-1}\left(\dfrac{V}{H}\right) - \sinh^{-1}\left(\dfrac{V - \dfrac{Gl_n}{L_0}}{H}\right)\right] \\ y_n = \dfrac{Gl_n}{EA_0}\left(\dfrac{V}{G} - \dfrac{l_n}{L_0}\right) + \dfrac{HL_0}{G}\left\{ \begin{array}{l} \left[1 + \left(\dfrac{V}{H}\right)^2\right]^{\frac{1}{2}} \\ - \left[1 + \left(\dfrac{V - \dfrac{Gl_n}{L_0}}{H}\right)^2\right]^{\frac{1}{2}} \end{array} \right\} \end{cases} \qquad (14)$$

4.2 Trajectory compensation considering the elastic catenary of the rope

When the lifting system performs a task that requires high accuracy of the suspended object, it ensures that the suspended object moves according to the expected trajectory through trajectory compensation. Trajectory compensation is to correct the position and posture error caused by the deformation of the rope, to enhance the safety and reliability of the lifting operation[20]. The kinematic theory and the compensation principle of position and posture are combined to establish the compensation model of the rope-driven parallel lifting system.

4.2.1 Compensation principle of position and posture

The configuration of the lifting system should be rationally arranged according to the requirements of the lifting task, and the movement of the barycenter of the moving platform should be planned according to the expected trajectory of the suspended object. Then, the expected trajectory of the ends of the three robots can be obtained according to the initial coordinates of the ends of the robots. Similarly, the movement trajectory of the suspended object can be obtained by planning the movement trajectories of the ends of the three robots. Considering the effect of the deformation of the rope on the movement of the suspended object, the movement trajectory of the suspended object is compensated by adjusting the end position of the robot.

The ends P_1, P_2 and P_3 determining plane of the three robots are defined as the moving platform, and the connection points B_1, B_2 and B_3 determining plane of the three ropes and the suspended object is defined as the static platform. As shown in Fig. 3, the coordinate system O_P is established at the barycenter of the moving platform, and the coordinate system O_B is established at the barycenter of the static platform. $\boldsymbol{p}_i$ is the vector pointing from the coordinate system O_B to the end of the robot, $\boldsymbol{b}_i$ is the vector pointing from the coordinate system O_B to the connection point between the rope and the static platform, and $\boldsymbol{L}_i$ is the rope vector.

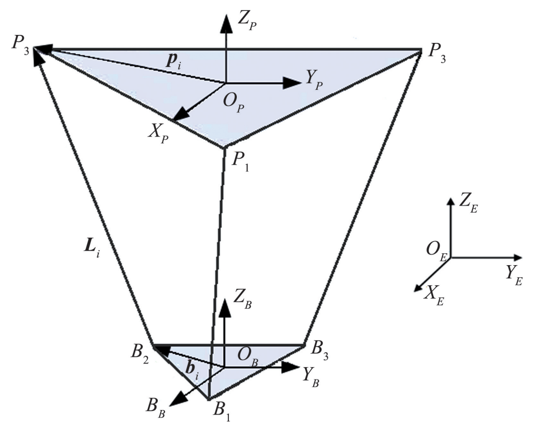

Fig. 3 Rope-driven parallel lifting system

The deformation of the rope will lead to changes in the position and posture of the static platform in the inertial coordinate system. To meet the requirements of lifting and reduce the movement deviation of the static platform due to the deformation of the rope, the movement trajectory of the static platform is compensated by adjusting the position and posture of the moving platform[21]. As shown in Fig. 3, the position and posture of the static platform satisfy the following requirements:

$$\boldsymbol{X}_{BP}^{P} = \boldsymbol{X}_{BE}^{E} + \boldsymbol{X}_{EP}^{P} \qquad (15)$$

$$\boldsymbol{R}_{B}^{P} = \boldsymbol{R}_{E}^{P}\boldsymbol{R}_{B}^{E} \qquad (16)$$

where, $\boldsymbol{X}_{BP}^{P}$ is the position vector of the static platform relative to the moving platform in the coordinate system O_P, $\boldsymbol{X}_{BE}^{E}$ is the position vector of the static platform relative to the inertial coordinate system in the inertial coordinate system O_E, $\boldsymbol{X}_{EP}^{P}$ is the position vector of the inertial coordinate system relative to the moving platform in the coordinate system O_P. The upper and lower scripts in Eq. (16) represent the same meaning.

According to the geometric relations in Fig. 3.

$$\boldsymbol{L}_i^P = \boldsymbol{p}_i^P - \boldsymbol{X}_{BP}^P - \boldsymbol{R}_B^P \boldsymbol{b}_i^B \tag{17}$$

where, $\boldsymbol{L}_i^P$ is calculated by Eq. (14), $\boldsymbol{b}_i^B$ is a known parameter. After the $\boldsymbol{X}_{BP}^P$ and $\boldsymbol{R}_B^P$ is obtained according to Eqs (15) and (16), $\boldsymbol{p}_i^P$ can be obtained, and the end position of each robot can be calculated.

When the elasticity and mass of the rope are considered in the lifting system, the expected trajectory of the static platform is known, as long as the position and posture of the moving platform relative to the static platform are solved, the deformation of the rope is compensated in real-time according to the calculation results by adjusting the end position of the robot, so that the rope is always tight under the gravity action of the suspended object, which can achieve the goal of position and posture compensation.

4.2.2 Trajectory compensation of multi-robot coordinated lifting system

As the driving part of the lifting system, the deformation of the rope will directly affect the position and posture of the suspended object. By compensating the deformation of the rope, the position and posture of the suspended object can be corrected. The goal of trajectory compensation is to ensure that the position and posture of the suspended object move according to the expected trajectory by adjusting the end position of the robot.

When the elasticity and mass of the rope are not considered, the relationship between the length of the rope and the position and posture of the suspended object is simply geometric. The kinematic equations of the lifting system are used to calculate the length of the rope. When considering the elasticity and mass of the rope, because the shape of the rope in the elastic catenary equation has a coupling relationship with the external force, the relationship between the length of the rope and the position and posture of the suspended object is no longer a simple geometric problem, but is closely related to the tension of the rope. Under the condition that only the end position of the robot changes, the expected position and posture of the suspended object are known, and the length of the rope under catenary deformation and elastic deformation superposed is calculated. Taking one of the ropes as an example, the principle of trajectory compensation of the lifting system is shown in Fig. 4.

Under ideal conditions, $\boldsymbol{P}_i$ is the expected position of the end of the robot, and $\boldsymbol{B}_i$ is the connection point between the rope and the suspended object. First, the mass and elasticity of the rope are not considered in the lifting process, the rope vector solved by inverse kinematics is $\boldsymbol{P}_i\boldsymbol{B}_i$, and the rope length calculated by Eq. (4) is l_i. Then considering the mass and elasticity of the rope, the actual position of the connection point between the rope and the suspended object is $\boldsymbol{B}_i^*$, the rope vector calculated by the elastic catenary equation is $\boldsymbol{P}_i\boldsymbol{B}_i^*$. φ is the angle between the rope before and after the deformation. To compensate for the movement error $\Delta \boldsymbol{B}_n$ of the suspended object, the compensation trajectory $\Delta \boldsymbol{P}_n$ of the end of the robot is obtained according to the compensation principle of position and posture. At this time, the rope vector is $\boldsymbol{P}_i^* \boldsymbol{B}_i^*$, and the rope length is calculated by Eq. (14).

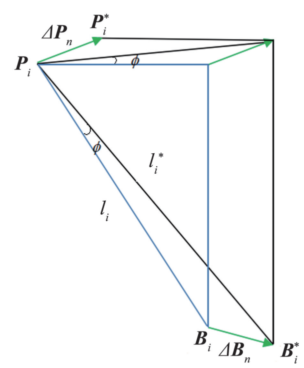

Fig. 4 Principle of the trajectory compensation

To make the movement trajectory of the suspended object as the desired trajectory, the movement error of the suspended object caused by the deformation of the rope is compensated by controlling the end position of the robot. Drawing on the establishment process of the elastic catenary equation of the rope, the calculus idea in mathematical analysis is introduced into the trajectory compensation of the lifting system. As shown in Fig. 5, the iterative method is adopted to solve the movement error $\Delta \boldsymbol{B}_n$ of the suspended object and the compensation trajectory $\Delta \boldsymbol{P}_n$ of the end of the lifting robot.

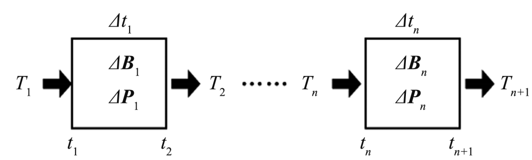

Fig. 5 The model is solved iteratively

The steps of the whole trajectory compensation are as follows.

(1) If the expected trajectory of the suspended object is known, the time domain t is divided into n e-

quidistant time steps Δt_1, Δt_2, $\cdots$, Δt_n. The rope deformation is not considered, the rope vector is $\boldsymbol{l}_1$, according to the inverse kinematics of the lifting system to calculate the position P_1, P_2, P_3 of the robot end in the inertial coordinate system. Using the kinematic and dynamic equation, the rope tension T_1 solved by Eq. (9) is taken as the initial value of the iteration, and the horizontal component H_1 and vertical component V_1 of the rope tension can be obtained.

(2) Considering the deformation of the rope, in the time step Δt_1, the rope tension T_2 can be solved by Eq. (12), the rope vector $\boldsymbol{l}_2$ can be solved by elastic catenary Eq. (14), the movement error $\Delta \boldsymbol{B}_1$ of the suspended object can be obtained through forward kinematics, and the compensation trajectory $\Delta \boldsymbol{P}_1$ of the end of the robot can be obtained by Eqs (15) – (17) according to the compensation principle of position and posture.

(3) In the time step Δt_2, according to the movement trajectory of the end of the robot, the position and posture of the suspended object, the rope tension is changed from T_2 to T_3, the rope vector is changed from $\boldsymbol{l}_2$ to $\boldsymbol{l}_3$, and the movement error $\Delta \boldsymbol{B}_2$ of the suspended object and the compensation trajectory $\Delta \boldsymbol{P}_2$ of the end of the robot can be obtained in the same way.

(4) According to the above calculation method, cycle to the $n+1$ step in succession until the movement error $\Delta \boldsymbol{B}_n$ of the suspended object and the compensation trajectory $\Delta \boldsymbol{P}_n$ of the end of the robot are calculated in the time step Δt_n, then the last moment t_{n+1} is the final movement result of the lifting system.

5 Simulation analysis

Assuming that the suspended object is a 200 kg cylindrical, the goal of the multi-robot coordinated lifting system is to have 200 kg the lifting capacity. The configuration of the three robots in the space is an equilateral triangular distribution, and the end positions of the three robots are always at the same height. The connection points between the suspended object and the ropes are distributed in an equilateral triangle, and the distance between the connection points and the barycenter of the suspended object is 1 m. The structure of the robot is $a_{i1} = 4$ m, $a_{i2} = 3$ m, $a_{i3} = 2$ m, and the coordinates at the bottom of the robot are $O_1(0,5,0)$, $O_2(-2.5\sqrt{3}, -2.5, 0.0)$, $O_3(2.5\sqrt{3}, -2.5, 0.0)$ respectively.

According to the requirements of the lifting task, it is assumed that the starting point of the lifting is $(0.0, 0.5, 1.0)$, the end point is $(0.5, 0.0, 3.5)$, the path planned in Descartes space is shown in Fig. 6, and the expected posture of the suspended object during the lifting is $(0,0,0)$. The initial values of the joint angles of each robot at the starting point are $\theta_{11} = -\pi/2$, $\theta_{21} = \pi/6$, $\theta_{31} = 5\pi/6$, $\theta_{i2} = \theta_{i3} = \pi/4$, and the joint angles of the subsequent path points are chosen from the inverse kinematics obtained from the previous path points. The joint parameters of the robot are shown in Table 1.

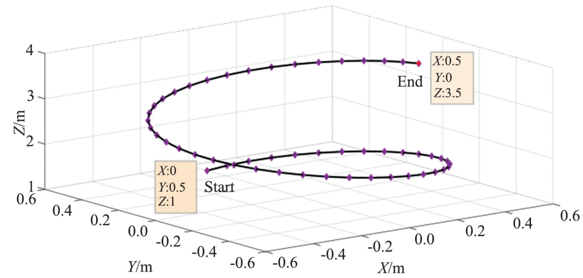

Fig. 6 The trajectory of the suspended object

Table 1 Parameter of the lifting robot

Parameter	θ_{11}	θ_{21}	θ_{31}	θ_{i2}, θ_{i3}
Value	$-\pi - 0$	$-\pi/4 - 3\pi/4$	$\pi/4 - 5\pi/4$	$\pi/12 - 5\pi/12$

Supposing that the driving mode of the lifting system is that only the position of the robot end changes, the rope length is 5 m, the elastic modulus of the rope is 1.8×10^5 MPa, the cross-sectional area is $2.54\ \text{mm}^2$, the mass per unit length of the rope is $0.58\ \text{kg} \cdot \text{m}^{-1}$, the minimum preload force of the rope is $T_{\min} = 100$ N, and the maximum allowable tension force is $T_{\max} = 1\,300$ N. The end positions of the three robots and the rope tension can be obtained by calculation, as shown in Figs 7 and 8.

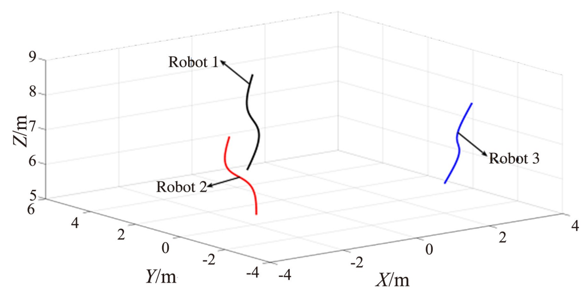

Fig. 7 End position of the robot

It can be seen from Fig. 7 that the end position changes are different for the three robots, but the movement curves of the robots are gentle, indicating that the robots run smoothly in the lifting process. As can be seen in Fig. 8, the tension changes in ropes 1

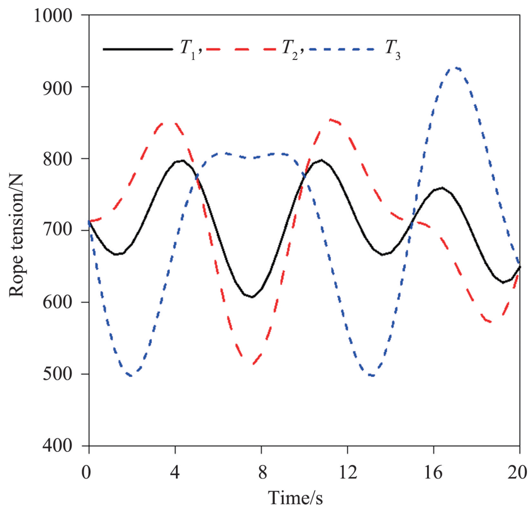

Fig. 8 The tension of the rope

and 2 are essentially the same. When the tension of rope 1 is in equilibrium with the internal forces, the tension of ropes 2 and 3 are the maximum and minimum, respectively, reflecting the law of the tension of the lifting system.

To evaluate the effect of trajectory compensation, the influence of rope deformation on the lifting system is analyzed through three working conditions. (1) The lifting is carried out without considering the deformation of the rope, and the resulting trajectory is the expected trajectory. (2) Under the same path, the deformation of the rope is considered. (3) Under the same path, the deformation of the rope is considered, and the movement trajectories of the lifting system are compensated. The movement trajectory of the suspended object can be obtained, as shown in Fig. 9. Figs 9 (a), (b) and (c) show the position of the suspended object, and Figs 9 (d), (e) and (f) show the posture of the suspended object, in the figures, solid line is expected trajectory, long dash line represents the trajectory considering the deformation of the rope, short dash line represents the trajectory considering the deformation of the rope and compensating.

Fig. 9 describes the effect of the rope deformation on the position and posture of the suspended object. When the deformation of the rope is taken into account, the movement trajectory of the suspended object fluctuates greatly after the compensated trajectory is closer to the expected trajectory of the suspended object, which shows the effectiveness of the compensation method, and also reflects that the influence of rope deformation on the position and posture of the suspended object can not be neglected. The average error of the position and posture of the suspended object is shown in Table 2.

Table 2 Average error before and after compensation

	X/m	Y/m	Z/m	α/°	β/°	γ/°
Before	0.317	0.108	0.395	5.694	3.927	2.315
After	0.186	0.039	0.125	1.764	1.478	0.489

It can be seen from Table 2 that after trajectory compensation, the average error in the Z direction is reduced from 0.395 m to 0.125 m, indicating that this compensation method can better compensate for the position error caused by the deformation of the rope, and meet the requirements of the control of the suspended object in the process of lifting. After trajectory compensation, the position and posture errors in the Z-direction are reduced by 68.35% and 78.88%, respectively, indicating that the deformation of the rope has a large impact on the movement of the suspended object.

To further observe the change law between the expected trajectory and the actual trajectory of the lifting robot, taking robot 1 as an example, the trajectories of the end of the robot and the tension of the rope are calculated. It can be found that the compensated trajectories are closer to the expected trajectories, which is consistent with the position and posture changes of the suspended object. The average error of the end position of robot 1 and the error of the rope tension are shown in Table 3.

Table 3 Average error before and after compensation

	X_{P1}/m	Y_{P1}/m	Z_{P1}/m	T_1/N
Before	0.421	0.289	0.356	30.504
After	0.268	0.089	0.079	15.674

It can be seen from Table 3 that the robot end has the largest error in the X-direction, which is related to the movement direction of the suspended object. To overcome the error caused by the deformation of the rope, the average error of the tension of the rope after compensation is reduced from 30.504 N to 15.674 N, which verifies the effectiveness of the compensation method. The average value of the rope tension is near the expected tension, and no rope failure occurs. If the planned end position of the robot and the rope tension are not corrected, the position and posture errors of the suspended object will become larger and larger over time, so the mass and elasticity of the rope must be considered in practical applications.

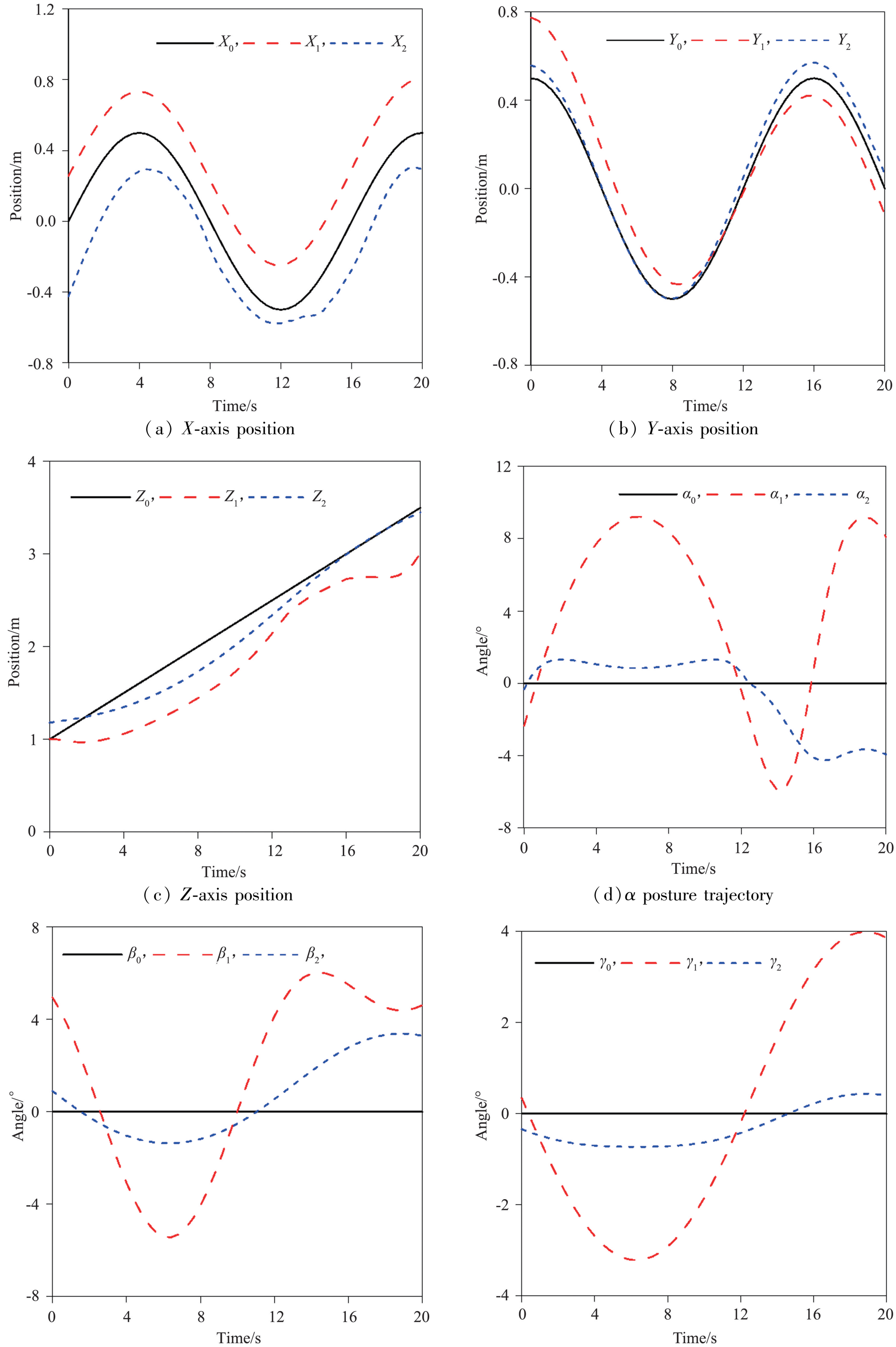

(a) X-axis position

(b) Y-axis position

(c) Z-axis position

(d) α posture trajectory

(e) β posture trajectory

(f) γ posture trajectory

Fig. 9 Trajectory of the suspended object

From the above simulated experiment, it can be seen whether or not the deformation caused by the mass and elasticity of the rope is considered has a large effect on the movement trajectory of the lifting system. After compensating for the deformation of the rope, the movement trajectory of the suspended object is closer to the expected trajectory. It shows that the rope deformation not only affects the movement error of the end of the robot but also affects the movement response of the suspended object, which verifies the necessity of trajectory compensation. If the trajectory compensation method is reasonable, the movement error of the suspended object can be reduced and the movement accuracy of the lifting system can be improved.

The Refs [7] and [8] analyzed the trajectory of rope-driven parallel robots from different perspective, the system has the number of ropes greater than or equal to the degree of freedom of the suspended object, and only considered the trajectory under dynamic conditions, while ignored the influence of the mass and elasticity of the flexible cables on the trajectories. The multi-robot coordinated towing system belongs to the unconstrained system. By analyzing the influence of the mass and elasticity of the ropes on the motion trajectory of the towing system, the results show that the proposed compenstion method can not only keep the tension and improve the distribution of the rope tension, but also ensure the accuracy of the towing operation. The research results are helpful for the multi-robot system to complete all kinds of towing tasks safely, and expand the related theory of rope-driven parallel mechanism.

6 Conclusion

According to the characteristics of the designed rope-driven multi-robot coordinated lifting system, the kinematic and dynamic models of the lifting system are established. The elastic catenary model of the rope is established, and the influence of the deformation of the rope on the position and posture of the suspended object is analyzed. The trajectory compensation method of the lifting system is proposed by using the compensation principle of position and posture. The iterative idea is used to solve the movement trajectory of the lifting system. The results show that whether or not the deformation of the rope is taken into account has a large effect on the trajectories, validating the need to take into account the elasticity and mass of the rope. At the same time, the proposed trajectory compensation method can significantly improve the motion accuracy of the lifting system, which validates the effectiveness of the compensation method.

References

[1] KIM E H, JUNG Y S, YU Y, et al. An advanced cargo handling system operating at sea[J]. International Journal of Control, Automation, and Systems, 2014, 12(4): 852-860.

[2] WANG L Q, XU Y G, HE N, et al. Modeling and simulation of flexible rope pendulum system excited by lifted object movement[J]. Journal of Shanghai Jiao Tong University, 2012, 46(9): 1416-1420. (In Chinese)

[3] PASSERINE C, ZANETTI D, MOSCHETTI G. Dynamic trajectory planning for failure recovery in cable-suspended camera systems[J]. Journal of Mechanisms and Robotics, 2019, 11(2): 1-10.

[4] SUI C P, ZHANG B, ZHAO M Y, et al. Modeling and control of a 3-DOF parallel wire-driven flexible manipulator[J]. Chinese Journal of Mechanical Engineering, 2005(6): 60-65. (In Chinese)

[5] HUANG P, ZHANG F, MENG Z, et al. Adaptive control for space debris removal with uncertain kinematics, dynamics and states[J]. Acta Astronautica, 2016, 128: 416-430.

[6] BEDOUSTANI Y B, TAGHIRAD H D, AREF M M. Dynamics analysis of a redundant parallel manipulator driven by elastic ropes[C]// International Conference on Control. Hanoi, Vietnam: IEEE, 2009: 536-542.

[7] ZHAO T, ZI B, QIAN S. Algebraic method-based point-to-point trajectory planning of an under-constrained cable-suspended parallel robot with variable angle and height cable mast[J]. Chinese Journal of Mechanical Engineering, 2020, 18(6): 33-54. (In Chinese)

[8] ZI B, DING H, CAO J, et al. Integrated mechanism design and control for completely restrained hybrid-driven based rope parallel manipulators[J]. Journal of Intelligent & Robotic Systems, 2014, 74(3-4): 643-661.

[9] YAN Y J, SHANG W W. Catenary model and dynamic analysis of a 6-DOF rope-driven parallel robot[J]. Journal of University of Science and Technology of China, 2015, 45(7): 546-554. (In Chinese)

[10] KORAYEM M H, BAMDAD M. Dynamic load-carrying capacity of rope-suspended parallel manipulators[J]. The International Journal of Advanced Manufacturing Technology, 2009, 44: 829-840.

[11] KORAYEM M H, YOUSEFZADEH M, BEYRANVAND B. Dynamics and control of a 6-DOF rope-driven parallel robot with visco-elastic ropes in presence of measurement noise[J]. Journal of Intelligent & Robotic Systems, 2017, 88: 73-95.

[12] KORAYEM M H, TAHERIFAR M, TOURAJIZADEH H. Compensating the flexibility uncertainties of a rope suspended robot using SMC approach[J]. Robotica, 2015, 33: 578-598.

[13] HE W K, FEI Y Q, CHEN M. Error analysis and compensation of rope-driven parallel robot[J]. Machinery Design & Manufacture, 2018(S2): 176-179. (In Chinese)

[14] RIEHL N, GOUTTEFARDE M, KRUT S, et al. Effects

of non-negligible rope mass on the static behavior of large workspace rope-driven parallel mechanisms [C]//IEEE International Conference on Robotics and Automation. Piscataway, USA: IEEE, 2009: 2193-2198.

[15] SU C, ZHAO X T, YAN Z Z, et al. Load stability analysis of a floating multi-robot coordinated towing system[J/OL]. Journal of Shanghai Jiao Tong University (Science), 2023. https://doi. org/10. 1007/s12204-023-2634-7.

[16] ZHAO X T, ZHAO Z G, WEI Q Z, et al. Dynamic analysis and trajectory solution of multi-robot coordinated towing system[J/OL]. Journal of Shanghai Jiao Tong University (Science), 2023. https://doi. org/10. 1007/s12204-023-2649-0.

[17] KHOSRAVI M A, TAGHIRAD H D. Dynamic analysis and control of cable driven robots with elastic cables [J]. Transactions of the Canadian Society for Mechanical Engineering, 2011, 35(4): 543-557.

[18] KIM Y K, KIM Y, JUNG Y S, et al. Developing accurate long-distance 6-DOF movement detection with one-dimensional laser sensors: three-beam detection system [J]. IEEE Transaction on Industrial Electronics, 2013, 60(8): 3386-3395.

[19] DU J L, BAO H, CUI C Z, et al. Dynamic analysis of rope-driven parallel manipulators with time-varying rope lengths[J]. Finite Elements in Analysis and Design, 2012, 48(1): 1392-1399.

[20] JIANG Y, TANG L, CHEN Y. Dynamics models of four degrees of freedom rope-driven rigid-flexible hybrid wave compensation device[J]. Journal of Central South University (Science and Technology), 2020, 51(7): 1767-1780. (In Chinese)

[21] HU Y P. Research on key technologies of design and control of parallel weave compensation system with six DOFs [D]. Changsha: National University of Defense Technology, 2017. (In Chinese)

ZHAO Xiangtang, born in 1995. He received the M. S. degree from Lanzhou Jiaotong University in 2022, he is now pursuing his doctorate at Lanzhou Jiaotong University. His current research interests are rope-driven parallel robots and multi-robots technology.